April 2015

Role of p53 in Extending Longevity in Untransformed Fibroblasts

Lucia R. Shumaker
Worcester Polytechnic Institute

Worcester Polytechnic Institute

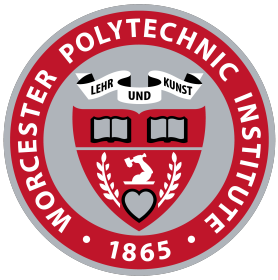

WPI

Role of p53 in Extending Longevity in Untransformed Fibroblasts

MAJOR QUALIFYING PROJECT REPORT
SUBMITTED TO THE FACULTY OF
WORCESTER POLYTECHNIC INSTITUTE
IN PARTIAL FULFILLMENT OF THE REQUIREMENTS FOR THE
DEGREE OF BACHELOR OF SCIENCE

Report Submitted To:
Associate Professor Tanja Dominko, Faculty Advisor

Submitted by:
Lucia Shumaker

April 30, 2015

1 Acknowledgements

I would like to thank the following individuals and organizations that helped make this project successful:

- Tanja Dominko and David Dolivo for their continued support and guidance throughout this project.
- Sarah Hernandez for her primers for p53 and p21 for RT-PCR reactions. David Dolivo for his qRT-PCR primers for p16 and MDM2.
- David Dolivo, Sarah Hernandez, and Olga Kashpur for their time, effort, and guidance.
- Paula Moravek and David Messier for providing training to work in the lab safely.

2 Table of Contents

3 List of Figures

4 Abstract

A better understanding of mechanisms that regulate cellular lifespan is needed to exploit the balance between senescence in normal cells and uncontrolled proliferation in cancer cells. We show that low oxygen and supplementation with FGF2 significantly extends cellular lifespan. Cells decrease expression of tumor suppressor p53 and p53 is downregulated further in late-passage cells. Lower levels of p53 protein accompany lower levels of transcription.

5 Introduction

5.1 The Cell Cycle and Its Regulation

All mammalian cells reproduce by progressing through a specific series of events to generate copies of their DNA and organelles prior to dividing into daughter cells that contain a full set of DNA and the complete organelle repertoire. This process, which regulates internal duplication and the subsequent division, is called the cell cycle. Each defined event in mitosis can be categorized by the portion of the cell cycle during which it occurs, and the cycle can be broken into four distinct phases: G_1, S, G_2, and M, and one additional possible phase, G_0, that the cell can enter if necessary (Cooper, 2000). G_1 and G_2 are growth phases in which the cell monitors the external environment and confirms that the cell is ready to proceed to the next phase. G_1 is the interval between cell division and S phase, during which the cell grows. G_2 follows S phase and is another period of cellular growth. The cell also synthesizes essential proteins for mitosis during G_2. S phase refers to the synthesis of DNA, because the cell replicates its genome during this phase. The actual division of the cell occurs during mitosis, or M phase, which follows G_2. M phase can be broken down into five more descriptive phases: prophase, metaphase, anaphase, telophase, and cytokinesis. During the first four of these phases nuclear division occurs, in which chromosomes (condensed DNA) align with their duplicates at the center of the cell and are segregated at either pole of the undivided cell. Once all has

been segregated appropriately, the cell begins cytokinesis and two daughter cells are formed, each with a complete genome (Alberts et al., 2008).

Figure 5.1 Regulation at cell cycle checkpoints controls how a cell progresses through the cell cycle.

Eukaryotic cells have a complex system of proteins that controls progression of the cell cycle and establishes checkpoints prior to moving from one phase to another. The cell-cycle control system ensures that the cell's DNA has been fully replicated, its mistakes corrected, and that each daughter cell is complete. If this biochemical checkpoint system fails, cells can continue dividing in the presence of replication errors or unrepaired mutations, potentially resulting in cancer (Alberts et al., 2008). One of the most important checkpoints in the eukaryotic cell cycle is the "restriction point," which occurs late in G_1. It functions as a decision point that regulates the

cell's passage into S phase and the rest of the cell cycle. A eukaryotic cell's passage through the restriction point is regulated predominantly by the presence of specific growth factors. If there is an absence of the appropriate growth factors, the cell will enter a quiescent stage, called G_0, during which it is still metabolically active but does not grow. A cell can escape G_0 if the necessary growth factors are provided. Eukaryotic cells must also pass checkpoints throughout the cell cycle that monitor DNA for damage. If damaged DNA is detected, the cell can be arrested during G_1 or G_2. A protein called p53 regulates arrest at the G_1 DNA damage checkpoint. Damaged DNA, as well as many other cellular stresses, activates p53 and causes it to initiate a cascade of events that halt the cell's progression through the cell cycle until the damaged DNA can be repaired (Cooper, 2000).

If DNA damage is sensed during G_1, ATM (ataxia telangiectasia, mutated; a serine/threonine protein kinase) phosphorylates several target proteins, including p53 and Chk2, which leads to two signal transduction pathways. One pathway is responsible for halting the cell cycle, and the other is responsible for maintaining the cell's halted state (Bartek and Lukas, 2001). When Chk2 is phosphorylated, it inactivates CDC25A by phosphorylation. Phosphorylation of CDC25A causes it to be excluded from the nucleus and degraded by ubiquitin-mediated proteasomal degradation (Molinari et al., 2000; Falck et al., 2001). This causes G_1 cell-cycle arrest, because if there is a lack of its target, CDC25A, inactive Cdk2 accumulates and it cannot phosphorylate the targets necessary for the cell to progress to the next phase. This form of cell cycle arrest signaling is called the ATM-Chk2-CDC25 pathway. UV damage-induced cell cycle arrest is signaled through the ATR-Chk1-CDC25 pathway (Sancar et al., 2004). In this pathway, ATR (ataxia telangiectasia and Rad3 related) or a similar protein kinase senses DNA damage and activates Chk1 by phosphorylation. Phosphorylated Chk1 can then phosphorylate CDC25A and therefore cause cell cycle arrest (Sancar et al., 2004). p53 maintains G_1/S cell cycle arrest after phosphorylation of Ser15 directly and Ser20 indirectly through activation of Chk1 or Chk2 by ATM or ATR (Banin et al., 1998; Canman et al., 1998; Kastan and Lim, 2000; Ryan et al., 2001; Chehab et al., 1999). The export of p53

from the nucleus for degradation is inhibited by phosphorylation. Therefore, during the maintenance of cell cycle arrest, p53 accumulates, leading to increased activation of its targets, including p21, a cell cycle inhibitor (Zhang and Xiong, 2001; Harper et al., 1993).

The activation of either of the ATM-Chk2-CDC25 or ATR-Chk1-CDC25 signal transduction pathways can initiate the halt of the cell cycle as DNA damage occurs during G_2 (Zhao and Piwnica-Worms, 2001; Xu et al., 2002; Brown and Baltimore, 2003). The alternate pathway to the initial pathway employed is responsible for maintaining cell cycle arrest following the initial signaling by the appropriate pathway for the type of DNA damage (Abraham, 2001; Xu et al., 2002; Brown and Baltimore, 2003).

Additionally, progression of the cell cycle is regulated by a family of proteins called cell division cycle (CDC) proteins. This family includes many classes, of which some are cyclins, cyclin-dependent kinases (CDK), mitogen-activated kinases, and phosphoprotein phosphatases (Nurse, et al., 1998). Cyclins have no enzymatic activity as independent proteins. They instead function by binding and activating CDKs. In order for CDKs to become enzymatically active, they must also be in a specified phosphorylation state. The specific pattern of phosphorylated and dephosphorylated residues determines the activity of the CDK. CDKs rely on other kinases and phosphatases to achieve appropriate phosphorylation. CDKs act by transferring phosphate groups from ATP to specific locations on their substrates. Cells rely on the appropriate phosphorylation of cyclin-CDK complex substrates at specific time points in the cell cycle to progress. Animals have varying numbers of CDKs, though vertebrates have four, CDK1, CDK2, CDK4, and CDK 6. The ability of CDKs to target multiple substrates comes from a variety of phosphorylation states and the binding of different cyclins. Each cyclin acts during a specific stage in the cell cycle and binds a single CDK. While CDK levels are kept relatively constant throughout the cell cycle, cyclin levels are modulated according to cell cycle phase by varying their manufacture and degradation (O'Connor et al., 2010).

5.2 Growth Factors and the Cell Cycle

Fibroblast growth factors (FGFs) are a family of mitogens that consists of 23 known members, and several splice variants, that have five known associated receptors (FGFRs). Mitogens are chemical substances that promote progression of the cell cycle, which are expressed in many tissues and cell types (Shaulian et al., 1997). FGF activity is regulated by tissue-specific heparin-sulfate proteoglycans (HSPGs). HSPGs can either activate or inactivate FGFRs by selective phosphorylation to modulate a cell's response to FGFs (Zhang, et al., 2006). Cellular responses to FGF signaling vary greatly and depend on the external environment, interactions with other growth factors, and the differentiation status of the cell (Coutu and Galipeau, 2011).

FGFs have been shown to play an essential role in embryonic development and are regulators of stem cell self-renewal and senescence (Coutu and Galipeau, 2011). It is believed that FGFs helps to maintain a balance between somatic stem cell progenitor pools and cells entering differentiation (Kassem and Marie, 2011). One member of the FGF family in particular, FGF-2, has been shown to contribute to the maintenance and self-renewal of pluripotency in human embryonic stem cells (hESCs). In differentiated cells, FGFs affect cell proliferation, differentiation status, and migration. Evidence presented in Coutu and Galipeau's review (2011) suggests that FGF acts in a permissive role to stimulate differentiation in committed cells by mediating cellular responses to other signaling molecules. FGFs appear to keep cells from senescing via extension of proliferative cellular lifespan.

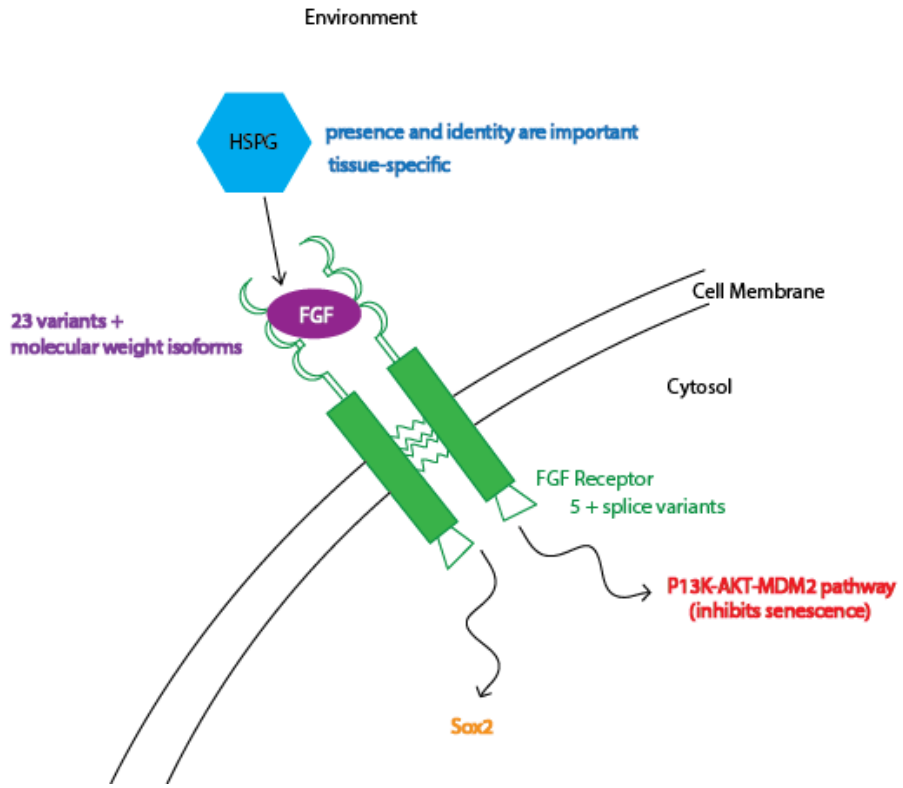

Figure 5.2 Interactions between HSPG, FGF, and FGFR induce signal cascade within the cell.

5.3 Senescence

Cellular senescence refers to the irreversible arrest of the cell cycle at G_1, during which cells become resistant and unresponsive to growth factor stimulation (Nakagawa and Opitz, 2007). Cells can typically undergo a limited number of population doublings before they enter senescence. This limited number of population doublings is termed the Hayflick limit. Most somatic human cells are capable of about 40 to 60 population doublings *in vitro* before they senesce (Hayflick and Moorhead, 1961). Stem cells and cancer cells do not have typical Hayflick limits. Both types of cells can divide indefinitely, though stem cells do so while maintaining stable karyotype, while cancer cells have escaped normal cell cycle regulation and can produce cells with increasingly damaged genomes.

The causes of senescence are often debated. It has yet to be established whether aging causes senescence, or whether senescence causes aging, though there is strong evidence to suggest that the two are often linked (Rodier and Campisi, 2011; Wright and Shay, 2002). Senescence can be triggered by both intrinsic and extrinsic factors (Itahana et al., 2004). Several cellular pathways have been implicated in the process of initiation of cellular senescence via intrinsic factors, including the p53/p21 and p16/pRb pathways (Itahana et al., 2004). The length of cellular telomeres has also been implicated in cellular aging. Telomeres are non-coding sequences at the end of eukaryotic chromosomes that protect the ends from recombination or non-homologous end joining, and they guide accurate replication of DNA at the end of chromosomes (Counter et al., 1992). Telomeres are shortened progressively with each cell division in somatic cells (telomere attrition) unless telomerase is present. Telomerase is a ribonucleoprotein complex that extends telomeres and is found in most human cancer cells, but is only expressed at low levels in healthy, terminally differentiated cells. If telomeres decrease to a critical size, a cell will cease to divide and will enter senescence. Herbert et al. (1999) demonstrated that inhibition of telomerase in cells containing active telomerase leads to telomere shortening and reduction of the cellular lifespan. The external environment can also contribute to the entrance of a cell into senescence. High oxygen concentration has been shown to trigger the p16 pathway in humans, which causes cell cycle arrest (Vijg and Campisi, 2008).

Researchers have been able to create immortalized cell line models in murine cells due to the cells' long telomeres. A cell line originating from a multicellular organism that has escaped cellular senescence by mutation or transformation is considered immortalized. Work has been done to immortalize human cells by transforming them with telomerase constructs (Counter et al., 1992). This procedure has been relatively successful in maintaining a cell's proliferation status, but it cannot rescue cells in which the p16 pathway has triggered cellular senescence (Coutu and Galipeau, 2011). Immortalized cell lines are immensely useful in cellular biology research because they allow researchers to continually study the same cell

population and can extend the lifespan of experiments. Unfortunately, immortalized cell lines are often susceptible to becoming cancerous (Vijg and Campisi, 2008) and we would like to develop long-lived or immortalized human cells that are not predisposed towards cancer for research and possible therapeutic applications.

5.4 p53 as a Player in the Cell Cycle

Eukaryotic cells must regulate their propagation and division in order to avoid accumulating deleterious mutations and undergoing cancerous transformation. Tumor suppressor protein p53 is one of the most rigorously studied proteins in this regulation network. p53 is activated by numerous cellular signals or conditions, including DNA damage, oxidative stress, osmotic shock, ribonucleotide depletion, and deregulation of oncogene expression. When p53 is activated, its N-terminal domain is phosphorylated at many residues and its half-life is increased dramatically. This allows for more p53 to accumulate in the cell. When the protein is phosphorylated, it also undergoes a conformational change that causes it to become an active transcriptional regulator. The phosphorylation of the N-terminal domain is crucial because this region is the primary target of the protein kinases that transduce stress signals. The targeting kinases can be grouped into two families, the MAP kinases that are responsible for cellular stress signals, and the remaining kinases that are responsible for genome integrity checkpoint signaling.

Additionally, p53 plays a significant role in mediating apoptosis (programmed cell death) and contributing to the establishment of cellular senescence (Shaulian et al., 1997). Over-expression of *TP53* is known to trigger apoptosis in cells and may do so if specific cellular factors are absent or if the cell senses excess activity of deleterious proteins. p53 is translated at higher rates upon genotoxic stress, and p53's target genes are selectively activated. These include *MDM2*, *BAX*, *WAF1/CIP1*, and *GADD45*. Interestingly, several splice variants of the MDM2 protein can bind p53 (Olson, 1993) and tag it for ubiquitin-mediated degradation. In this way, MDM2

activity can modulate p53 activity and form a negative feedback loop, though complexes of MDM2 and p53 are not always detectable in cells co-expressing the two genes. The negative regulation of p53 allows cells to keep p53 levels in check (Shaulian et al., 1997). Overexpression of *MDM2* has been used to immortalize cell lines (Finlay, 1993) and can rescue cells from p53-triggered senescence (Chen et al., 1996; Haupt et al., 1996).

The human *TP53* gene encodes a full-length protein of 393 amino acids (GenBank: BAC16799.1, NCBI, NIH), and it is relatively well conserved between mammalian species (Walker et al. 1999). The gene has been mapped to human chromosome 17. Binding of p53 to DNA can stimulate *CDKN1A*, the gene encoding p21, which has also been linked to intrinsic triggering of cellular senescence (Coutu and Galipeau, 2011). p21 and a cell division kinase (Cdk2) interact to inhibit the cell's progression to the next stage of the cell cycle. In the absence of functional p53, transcription of p21 is not activated, and cells can escape the cell cycle checkpoints for appropriate cell division. For a summary of p53's interaction network and the cellular stresses that activate it, see Figure 5.3.

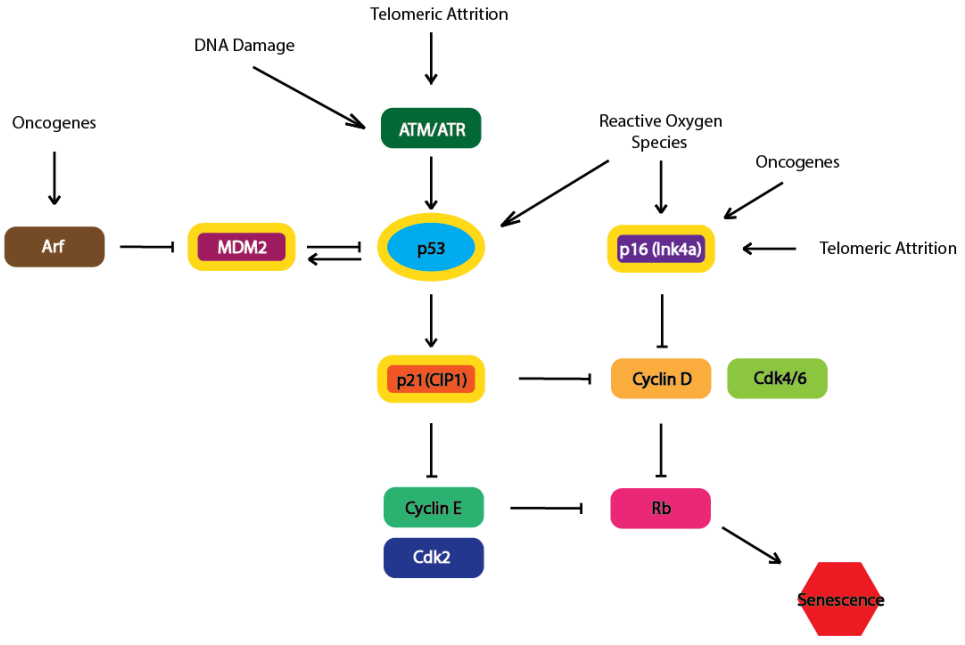

Figure 5.3 p53 interaction network and pathways to senescence.

5.5 Extending Lifespan in Differentiated Human Cells

Research has shown that human somatic cells can respond to manipulation of oxygen concentration and supplementation with FGF2 via up-regulation of some genes associated with pluripotency. These genes include *LIN28*, *Rex1, POU5F1* (OCT4 protein), *SOX2*, and *NANOG* (Page et al., 2009).

Previous studies by Takahashi, et al. (2007a and b) showed that transfection of human fibroblasts with genes for stem cell-associated transcription factors is sufficient to induce reversion to a pluripotent state. The transfection of cells with transcripts for *POU5F1, SOX2, NANOG*, and *LIN28* and subsequent activation of the genes seems to be enough to begin the process of returning cells to pluripotency and for the expression of embryonic stem cell characteristics (Yu et al, 2007; Page et al., 2009).

Our lab has shown that fibroblasts grown in a humidified environment at 37˚C and 5% O_2, 5% CO_2, and 90% N_2 and in media supplemented with FGF-2 were able to undergo 70 population doublings over their proliferative lifespan. A control population of fibroblasts grown in atmospheric oxygen concentration (19%) and without FGF-2 only underwent 33 population doublings by comparison (Page et al., 2009). The conditions described for the experimental group (5% O_2 and FGF-2) have been termed induced regeneration competent *(*iRC) conditions and will be referred to as such throughout this project (Kashpur et al., 2013). The cells are referred to as "regeneration competent" because they express stem-cell marker genes and are therefore demonstrate phenotypes associated with cellular plasticity. Therefore, they are responsive to signals that stimulate reentry into the cell cycle (Stocum, 2002) and may participate in regenerative tissue healing (Page et al., 2011).

The ability to return differentiated somatic cells to a more plastic state has significant implications for development of patient-specific cells for therapy and

new models for disease progression research (Page et al., 2009). Our lab has been able to produce iRC cells from terminally differentiated human dermal fibroblasts; bringing us a step closer to useful applications of developmentally plastic cells. The aim of the project was to investigate factors that may play a role in extended lifespan of iRC cells. A better understanding of these factors will help us identify molecular mechanisms regulating the switch between extended life span and immortalization during oncogenic transformation, bringing us closer to producing therapeutically relevant, non-tumorigenic autologous cell sources and replacing the need for embryonic stem cells for cell therapy.

I investigated the relative protein abundance of tumor suppressor protein p53 throughout the lifespan of iRC cells to determine whether the cells' extended life span was paralleled by a decrease in p53-mediated cellular senescence signaling. To achieve this goal, human fibroblasts were grown under iRC conditions (as defined above and described in Page, et al., 2009) and partial iRC conditions (either low oxygen concentration or supplementation with FGF2) and total protein and RNA collected during the first 30 days of exposure to a particular set of culture conditions. I was unable to collect samples during the later portions of the cells' *in vitro* lifespans due to the time limitations of the project. These samples were used for determination of p53 transcript by RT-PCR and qRT-PCR, and for determination of p53 protein levels by Western blotting p53. Results were compared to samples gathered from fibroblasts grown under control culture conditions (19% O_2 and with media not supplemented with FGF2). We hypothesized that p53 protein levels would rise with increasing population doublings in iRC cells in a similar pattern to the accumulation of p53 in control cells, though it would take longer to accumulate to comparable levels. In addition to p53, I investigated levels of p53-regulator MDM2 and levels of two G1/S phase cell cycle inhibitors, p21 and p16.

6 Materials and Methods

6.1 Cell Culture

Human dermal fibroblasts CRL-2352 cells were purchased from American Tissue Culture Collection (ATCC; Manassas, VA). This dermal fibroblast cell line was derived from a skin biopsy from a below-the-knee amputation conducted on a 24-year-old, Caucasian male suffering from lymphoma, though the tissue of origin was unaffected. The ATCC cell line description states that CRL-2352 cells typically senesce after about 32 population doublings, and the purchased cells had undergone three population doublings beyond their primary derivation.

Cells were grown in human dermal fibroblast (hDF) medium consisting of DMEM:Ham's F12 (50:50, MediaTech) with 10% Fetalclone III (Hyclone, Logan, UT). Prior to use, the DMEM (without L-Gln or phenol red) was supplemented with 4 mM fresh L-Gln (MediaTech, Manassas, VA). The four experimental culture conditions were as follows:

1. hDF medium placed in ambient oxygen (19%)
2. hDF medium supplemented with 4 ng/mL recombinant human fibroblast growth factor (FGF-2) (Chemicon, Temecula, CA, or Protide, Lake Zurich, IL) placed in ambient oxygen (19%).
3. hDF medium placed in 5% oxygen
4. hDF medium supplemented with 4 ng/mL recombinant human fibroblast growth factor (FGF-2) (Chemicon, Temecula, CA, or Protide, Lake Zurich, IL) placed in 5% oxygen.

Cells were seeded at 100,000 cells per 60-mm dish (Nunclon) at each passage and media was replaced every fourth day if the cells were not yet confluent. When cells were passaged, the media was aspirated from the plate, the cells were rinsed with PBS (Corning Cellgro, Manassas, VA), and then the cells were then incubated in trypsin (Corning Cellgro, Manassas, VA) at 37˚C for 5 minutes. The cells and trypsin were then mixed with fresh media, and the cell concentration was determined by

counting an aliquot of the mixture with a haemocytometer. At each possible passage, the cells remaining after plating were centrifuged at 10x*g* for 5 minutes, media aspirated, and the pellet resuspended in PBS. The centrifugation was repeated and the PBS wash was aspirated. The resulting cell pellet was then snap frozen by dipping the centrifuge tube containing it in liquid nitrogen. Once pellets were frozen, they were stored at -80˚C until the pellets were used for RNA or protein isolation.

6.2 RNA Isolation

Total RNA was isolated from cell pellets using Trizol following the manufacturer's protocol (Life Technologies). Trizol was added to sample pellets and the mixture was passed repeatedly through a 25-gauge syringe to break up the pellet. The addition of chloroform, agitation, and then centrifugation separated the mixture into the expected three phases: phenol-chloroform, interphase, and aqueous phases. The aqueous phase was isolated and used for RNA precipitation. Precipitation was induced by addition of isopropanol and isolated by centrifugation. The resulting pellet from the most recent centrifugation was saved and washed with ethanol, vortexed, and dried briefly. The RNA was resuspended in 25 µL of deionized water and its concentration was determined using the NanoDrop spectrophotometer.

6.3 Reverse Transcriptase Polymerase Chain Reaction (RT-PCR)

Complementary DNA (cDNA) was synthesized using Quanta BioSciences' qScript cDNA SuperMix according to the manufacturer's protocol. Reagents and 1 µg of RNA were combined for each 20-µL reaction in 0.2 mL micro-tubes and incubated in a thermocycler according to the manufacturer's specifications (Quanta BioSciences). cDNA was amplified using PCR with GoTaq DNA Polymerase (Promega). All RT-PCR reactions had a final concentration of 200 nM of each primer. Sequences of primers used are described in Table 6.1. The samples were held at 95˚C for 5 minutes, at a primer-specific annealing temperature (54˚C -60˚C) 15 seconds, 72˚C for 30 seconds

and the cycle repeated 29 times. After terminal extension at 72˚C for 7 minutes, the samples were held at 4˚C until analyzed. Samples were run on a 1.5% agarose gel in TAE buffer with ethidium bromide at 100 V. The gel was imaged with a BioRad Image Station.

Table 6.1 RT-PCR primer design and cycling conditions.

Primer	Forward Primer Sequence	Reverse Primer Sequence	Annealing temperature
p53	5'-CTC AGA TAG CGA TGG TCT GGC-3'	5'-GCC CAC GGA TCT GAA GGG-3'	54˚C
p21	5'-CCG AAG TCA GTT CCT TGT GGA G-3'	5'-CAA GGG TAC AAG ACA GTG ACA GG-3'	54˚C
Actin (Loading Control)	5'-TCT GGC ACC ACA CCT TCT ACA A-3'	5'-CTT CTC CTT AAT GTC ACG CAC G-3'	58˚C

6.4 Quantitative Reverse Transcriptase Polymerase Chain Reaction (qRT-PCR)

The cDNA was also used for amplification with for quantitative qRT-PCR and with Power SYBR Master Mix (Life Technologies). PCR conditions were suggested by the manufacturer's protocol. Primer sequences are shown in

Table 6.2. Cycling conditions were as follows: 95˚C for 10 minutes, 95˚C for 15 seconds, 60˚C for 1 minute, Repeat steps 2-3 40 times, Melt curve, Hold at 4˚C.

Table 6.2 qRT-PCR primer design and specifications.

Primer	Forward Primer Sequence	Reverse Primer Sequence	Annealing Temperature
p53	5'-GTG TTT GTG CCT GTC CTG GGA G-3'	5'-GCT CTC GGA ACA TCT CGA AGC C-3'	60˚C
p21	5'-CAC TGT CTT GTA CCC TTG TGC C-3'	5'-TTC CTC TTG GAG AAG ATC AGC CG-3'	60˚C
p16	5'-GAG CAC TCA CGC CCT AAG-3'	5'-AGT GTG ACT CAA GAG AAG CCA G-3'	60˚C
MDM2	5'-CCT TCT GAT CCT TAG TTT CTC TCT CC-3'	5'-TCA TTT ACA TAG CAC CAA ATA TAA GAG CC-3'	60 ˚C
Actin (Loading Control)	5'-AGA GCT ACG AGC TGC CTG AC-3'	5'- GGA TGC CAC AGG ACT CCA-3'	60˚C

For qRT-PCR analysis, the C_t values for the gene of interest were normalized relative to the C_t values for actin in order to account for differences in amount of cDNA template loaded (delta C_t). The delta C_t values were compared relative to the untreated control (ambient oxygen: 19%, no FGF2) in order to calculate the change in transcript expression levels conferred by each treatment.

6.5 Protein Isolation and Western Blotting

Total protein was isolated from fibroblast cell pellets with DK cell lysis buffer (5X stock: 200 mM Tris pH 7.5, 750 mM NaCl, 40% glycerol, 0.0626% Triton X-100, 0.025% Tween 20, 0.1% NP-40) supplemented with complete protease inhibitor cocktail (PIC, Santa Cruz Biotechnology) and sonication of the sample on ice. Protein concentration was determined with the Bradford assay kit, according to the

manufacturer's protocol (Thermo Scientific). Protein concentrations were determined using the "Standard Microplate Protocol" in a 96-well format. Absorbance readings for each of the samples were imported to Microsoft Excel and normalized by subtracting the absorbance of the blank standard.

$$normalized\ sample\ absorbance = (sample\ absorbance) - (blank\ absorbance)$$

The normalized sample absorbances of the standards were graphed versus the protein concentrations. Protein samples with unknown concentrations were assigned arbitrary values to visualize which dilution of the sample was most appropriate for the linear range of the standard curve. This can be seen in **Error! Reference source not found.** and **Error! Reference source not found.**. Two figures and two standard curves were generated because there were too many samples for a single 96-well plate.

Equal amounts of protein lysate and denaturing 2X sample buffer (BioRad Laboratories) were mixed and heated to 100˚C for 5 minutes prior to using the sample for gel electrophoresis.

Proteins were separated on 12% SDS-PAGE gels and transferred to PVDF membranes (BioRad Laboratories) using Towbin's transfer buffer (25 mM Tris, 192 mM glycine, 20% methanol, and 0.037% SDS). The membranes were blocked with Tween-Tris-buffered saline (TBS-T: 25 mM Tris, 137 mM NaCl, 2,7 mM KCl, 0.2% Tween), and 5% dry milk. 1% milk in TBS-T was used for primary and secondary antibody incubations. Primary mouse antibodies against p53 (Santa Cruz Biotechnologies) and rabbit antibodies against actin (Sigma) were used. Between antibody incubations, membranes were washed three times with TBS-T. Primary antibodies were detected with HRP-conjugated goat anti-mouse and anti-rabbit secondary antibodies, respectively, and signal detected by chemiluminescence (Luminol; Santa Cruz Biotechnologies). Images were obtained with a BioRad Image

Station and the intensities of bands were quantified using densitometry analysis in ImageJ software.

6.6 Flow Cytometry

Cells were pelleted as before to wash out media and resuspended in 70% ethanol for fixation prior to performing flow cytometry on the samples. Samples were then treated with RNase A and stained with propidium iodide according to the protocol written by Piotr Pozarowski and Zbigniew Darzynkiewicz, "Analysis of Cell Cycle by Flow Cytometry".

The flow cytometry events corresponding to fragments of DNA, particulate matter, and cellular debris were excluded from analysis based on their low fluorescence (565-605 nm range, FL-2 channel). The remaining events were assumed to be derived from cells living at the time of fixation. Signals recorded from the FL-2 channel were plotted as event count as a function of FL-2 intensity.

7 Results

7.1 Population Doublings of Fibroblasts Cultured Under Different Conditions

Human dermal fibroblasts (CRL-2352) were grown under the following experimental conditions: hDF media without FGF2 and in 19% O_2, hDF media without FGF2 and in 5% O_2, hDF media with FGF2 and in 19% O_2, and hDF media with FGF2 and in 5% O_2. The concentration of cells was determined by counting cells using a 0.1-mm Haemocytometer at each passage. Cell counts were recorded and Microsoft Excel was used to calculate the cumulative population doublings each cell population had undergone at each passage (Figure 7.1). The calculations for population doublings were performed using the following formulas:

Concentration of cells on plate to be passaged:

$$\frac{Cells}{mL} = (\#\ of\ cells\ counted)/4 * 10{,}000$$

Total Number of cells on plate to be passaged:

$$Total\ \#\ of\ Cells = \frac{cells}{mL} * (volume\ of\ media\ on\ plate\ to\ be\ passaged)$$

Number of population doublings since the previous passage:

$$Population\ Doublings\ = \frac{ln\left[\frac{Total\ \#\ of Cells}{\#\ of\ Cells\ Plated\ at\ Previous\ Passage}\right]}{ln(2)}$$

Population doubling rate since the previous passage:

$$Population\ Doubling\ Rate = \frac{Population\ Doublings}{Days\ Since\ Previous\ Passage}$$

Cumulative population doublings:

$$Cumulative\ Population\ Doublings$$
$$= \Sigma(Population\ Doublings\ from\ all\ previous\ passages)$$

Treatment with FGF2 and low oxygen started after 18 days in culture (designated Day 0). Samples for RT-PCR, qRT-PCR, and Western blotting were collected on Days 7, 18, 21, 22, 27, 32, and 34 after treatment began. The cell populations were still growing and continued to be passaged, though they had begun to exhibit phenotypic characteristics of senescent cells, including becoming increasingly vacuolated.

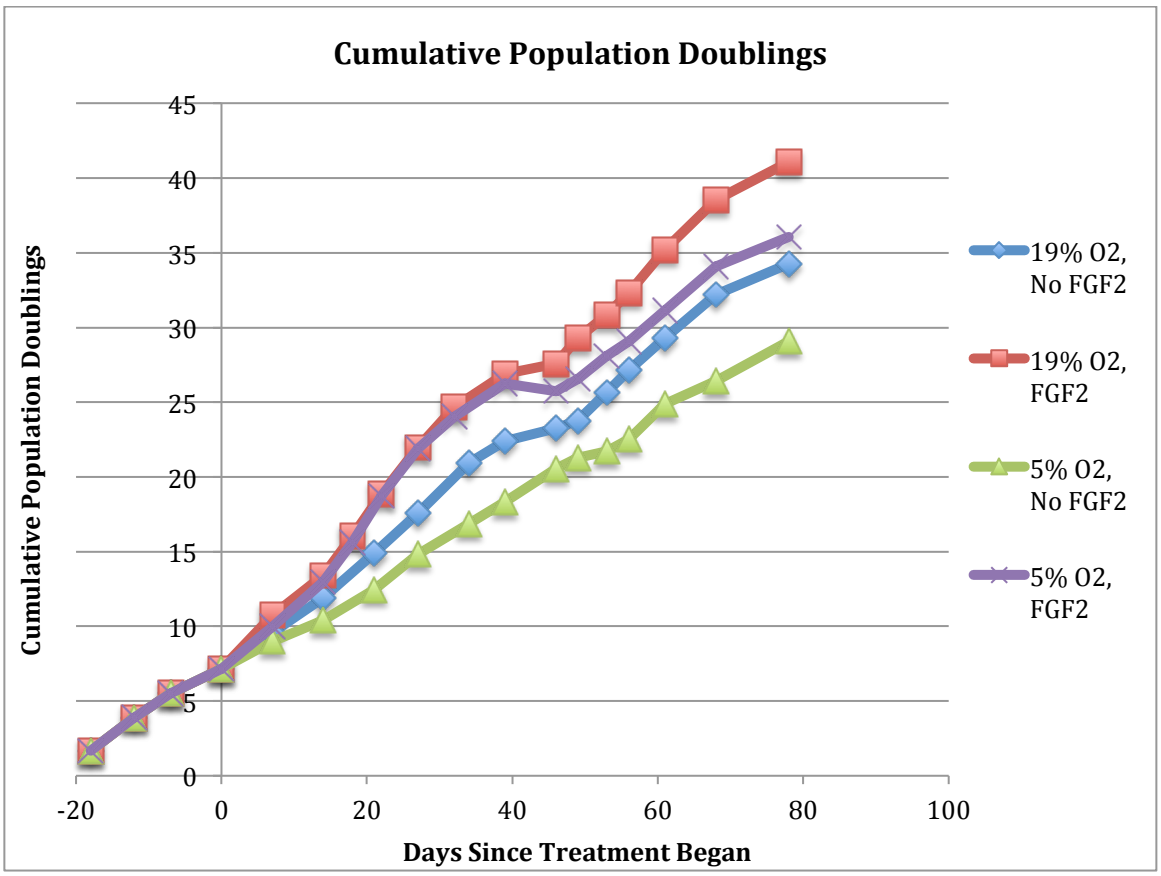

Figure 7.1 Cumulative population doublings of fibroblasts grown under the four experimental conditions.

After 32 days in treatment, the cells cultured in 19% O_2 with FGF2 had undergone 24.68 population doublings and the 5% O_2 + FGF2 cells had undergone 24.01 doublings. After 34 days in treatment, the 19% O_2 cells (without FGF2) had undergone 20.95 doublings, and the 5% O_2 cells (without FGF2) had only undergone 16.89 doublings. The slight dipping in the lines in Figure 7.1 are likely due to the effects of freezing the cells in liquid nitrogen (for a time period when I was unable to be at school and take care of them). At the time point recorded, samples of cells were fixed in preparation for performing flow cytometry. The cells had undergone the following numbers of population doublings by the end of the experiment: 19% O_2 without FGF2, 34.28; 19% O_2 with FGF2, 41.09; 5% O_2 without FGF2, 29.08; 5% O_2 with FGF2, 36.08. Based on the findings described in Page, et al., 2009, the rate at which the populations treated with FGF2 double would be expected to diverge at

later passages. The combination of supplementation of media with FGF2 and growth in low oxygen concentrations increased the rate that a cell progressed through the cell cycle. Supplementation of media with FGF2 was sufficient to increase the rate at which the cells divided, while culturing at a lower oxygen concentration reduced the population-doubling rate (Figure 7.1).

7.2 mRNA Expression of p53 and p21 in Human Dermal Fibroblasts Grown Under Different Conditions

Total RNA was isolated from cell pellets harvested during the treatment time course, cDNA was synthesized, and RT-PCR was run for p53, p21, and actin (load control) (Figure 7.2).

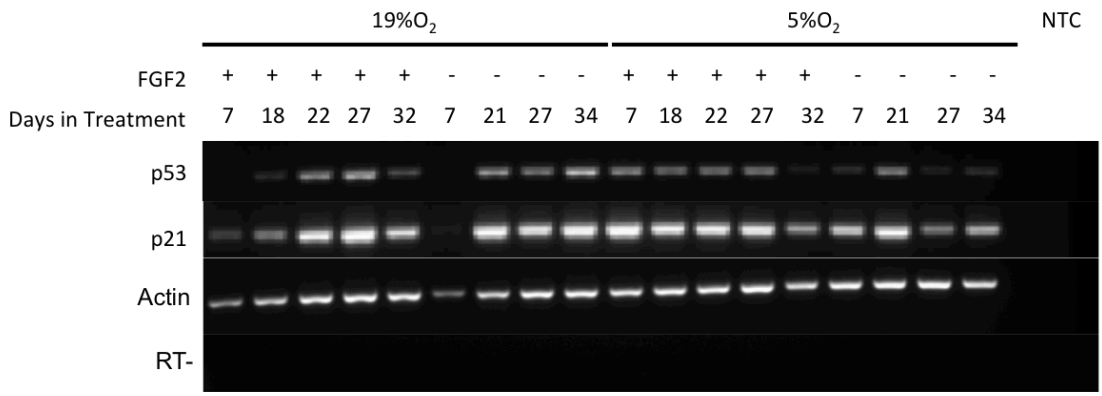

Figure 7.2 RT-PCR for p53, p21, and actin. No template control (NTC) and reverse transcriptase negative (RT-) controls are shown.

Transcript levels of p53 appear to accumulate over time and then be degraded or down regulated in older cells treated with FGF2, while untreated cells continue to accumulate p53 mRNA transcripts. Relative p21 transcript levels appear relatively constant throughout the time course studied.

The same cDNA samples were also used in performing qRT-PCR for p53, p21, MDM2, and p16 (Figure 7.3, Figure 7.4, Figure 7.5, and Figure 7.6). The expression

fold change of each gene of interest was normalized to the first sample (Day 7) and to actin.

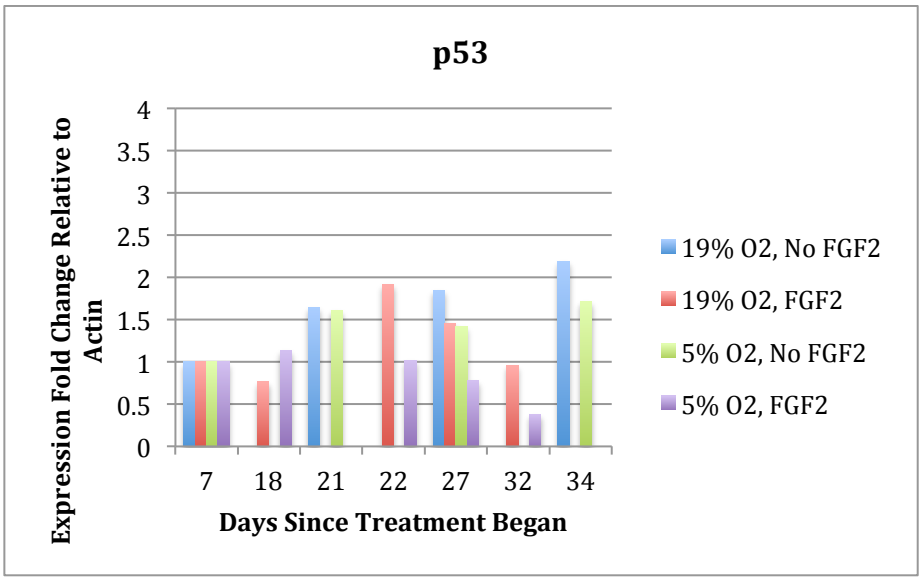

Figure 7.3 Analysis of the qRT-PCR for p53 represented as the fold change in p53 expression relative to actin.

Transcript levels of p53 accumulate over time in control cells, while expression appears to be down regulated in iRC cells. There is a possible, low peak in p53 levels at Day 18 in the iRC cells, though this should be evaluated in greater detail in further, replicate studies. p53 transcript levels are lower overall in cells cultured in lower oxygen than in control cells. Treatment with FGF2 appears to reduce transcript levels of p53 in later passage cells compared to control cells, but the reduction in p53 transcript took longer.

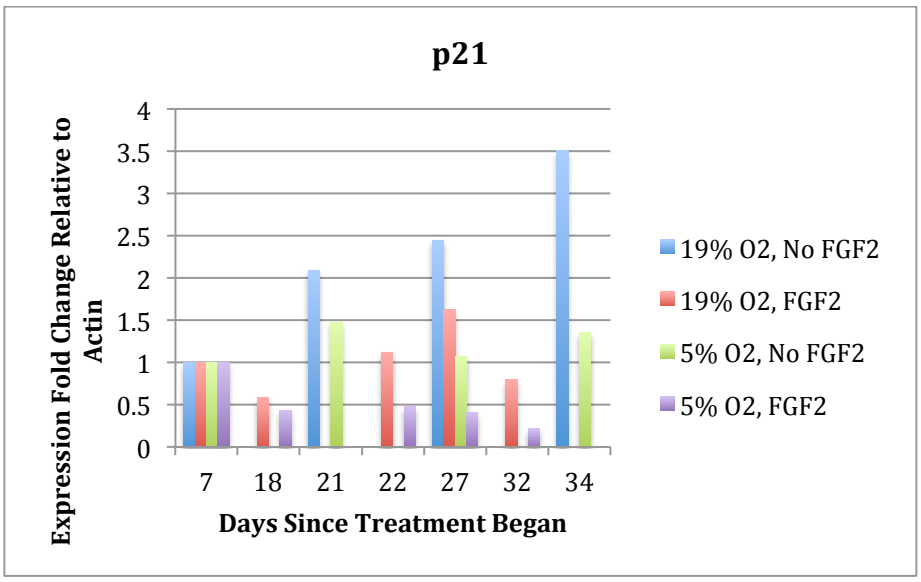

Figure 7.4 Analysis of the qRT-PCR for p21 represented as the fold change in p21 expression relative to actin.

p21 transcript levels followed similar trends to p53 transcript levels in all the culture conditions. p21 transcripts accumulate over time in control cells and exhibit a down regulation in iRC cells. Reducing the oxygen concentration caused lower, though roughly steady, levels of p21 transcript. Addition of FGF2 to culturing media appears to delay accumulation of p21 transcripts and then cause a later down regulation.

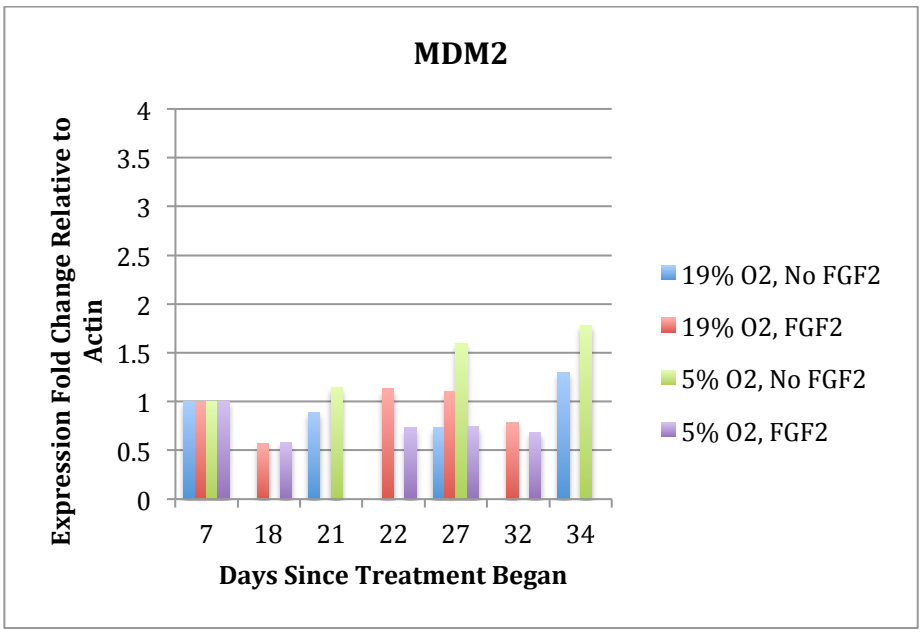

Figure 7.5 Analysis of the qRT-PCR for MDM2 represented as the fold change in MDM2 expression relative to actin.

MDM2 transcript levels did not exhibit similar trends to p53 or p21. There are no particular trends down or upwards of MDM2 transcript levels under three of the four culture conditions. The only culture condition to exhibit a trend was a slow accumulation of MDM2 transcript in the 5% O_2 cells without FGF2.

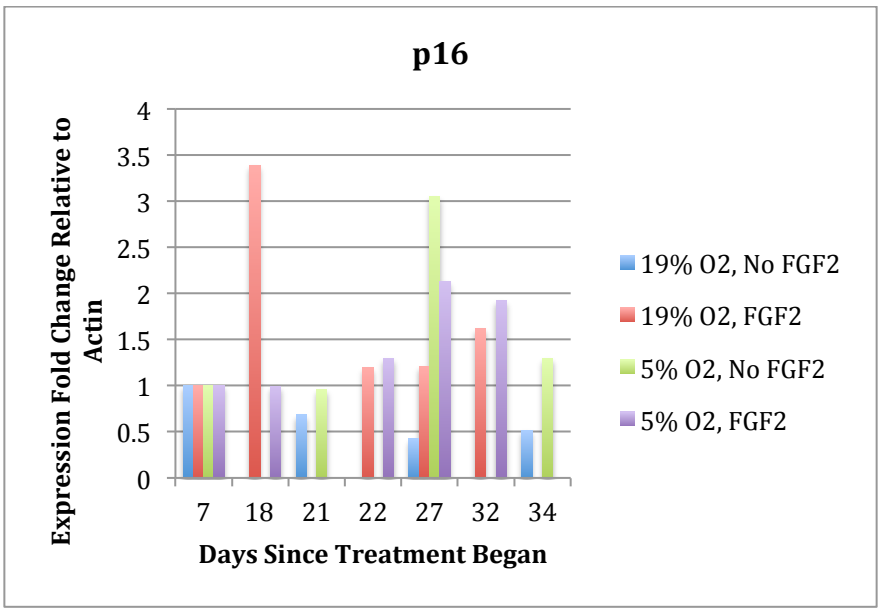

Figure 7.6 Analysis of the qRT-PCR for p16 represented as the fold change in p16 expression relative to actin.

Similar to MDM2, p16 transcript levels did not appear to follow particular trends in three of the four culture conditions. 5% O_2 + FGF2 appears to cause p16 transcript to accumulate and then be down regulated at the latest time point. This trend is noted because it is similar to the trend seen in p53 and p21 transcripts at certain culture conditions.

The results of the qRT-PCR show that p53 and p21 mRNA transcripts accumulate at the highest rate in 19% O_2 cells untreated with FGF2. iRC cells show a reduction in p53 and p21 transcript levels over time. The partial iRC conditions show lower levels of p53 and p21 transcript than control cells. It appears that FGF2 may contribute to the downward trend over time of p53, while lower oxygen concentration reduces the accumulation rate. MDM2 and p16 were not expected to follow the same patterns as p53 and p21, since they are regulated in different manners. Neither demonstrates a coherent trend during the time course studied.

7.3 Levels of p53 Protein in Human Dermal Fibroblasts Grown Under Different Conditions

Total protein was isolated from cell pellets harvested at the same time points used for the RNA. The normalized sample absorbances of the standards were graphed versus the protein concentrations. Protein samples with unknown concentrations were assigned arbitrary values to visualize which dilution of the sample was most appropriate for the linear range of the standard curve.

This can be seen in Figure 7.7 and Figure 7.8. Two figures and two standard curves were generated because there were too many samples for a single 96-well plate.

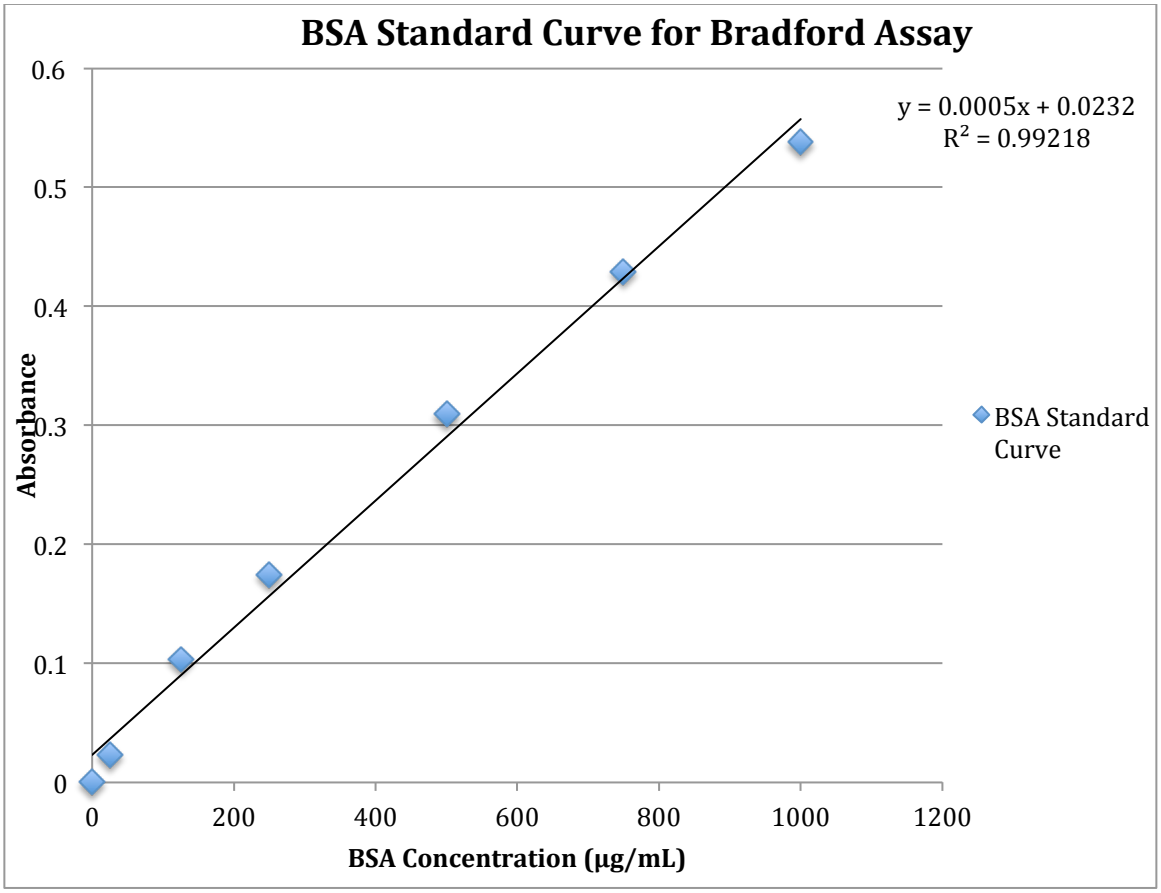

Figure 7.7 Bradford standard curve for the first of two plates run to determine sample protein concentrations. Y=0.0005x+0.0232; R^2=0.99218.

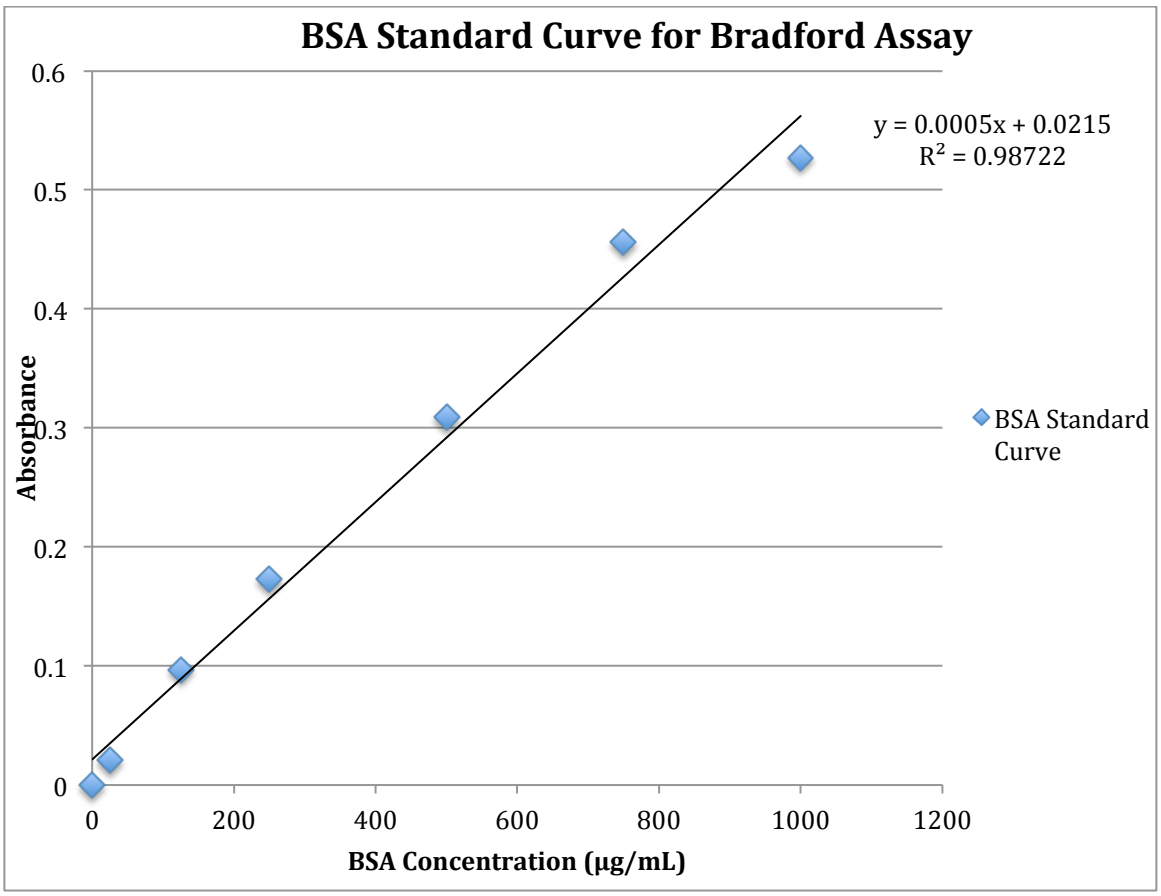

Figure 7.8 Bradford standard curve for the second of two plates run to determine sample protein concentrations. Y=0.0005x+0.0215; R^2=0.98722.

Protein levels were standardized prior to loading on SDS-PAGE gels, and Western blots were performed for p53 and actin (load control) (Figure 7.9 and Figure 7.10).

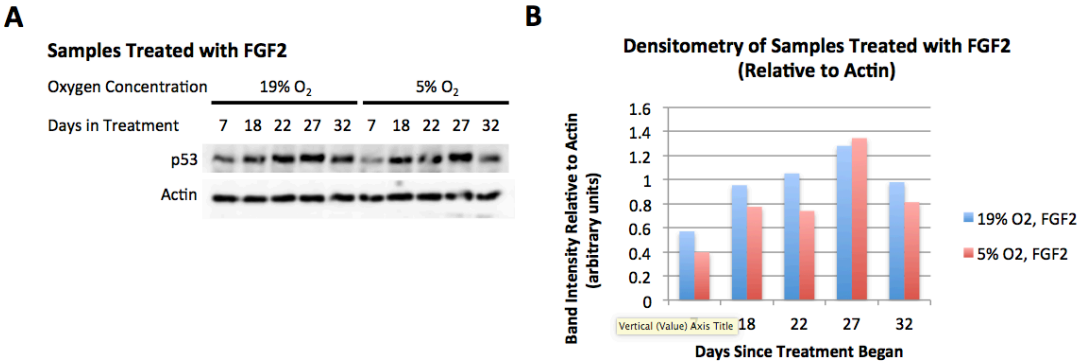

Figure 7.9 A) Western blot for p53 and actin control in cells treated with FGF2. B) Densitometry quantification of p53 Western blot results for samples not treated with FGF2. Values are calculated relative to actin.

Each sample was loaded with a relatively consistent amount of protein (see actin bands). p53 appears to accumulate over time in samples without FGF2, while the samples with FGF2 show the same drop in protein expression at the final time point that was noted in the qRT-PCR (Figure 7.3). The lower oxygen samples appear to have reduced levels of protein compared to the higher oxygen samples in both the presence and absence of FGF2.

The results of the Western blots in Figure 7.9A and Figure 7.10A were quantified using densitometry analysis and ImageJ software (Figure 7.9B and Figure 7.10B). The reduction of culture oxygen concentration in cells treated with FGF2 appears to lower p53 protein concentration at most time points relative to cells cultured in ambient oxygen. Both treatment conditions treated with FGF2 exhibit an increase in p53 protein concentration until the final time point sampled, when p53 protein levels drop (Figure 7.9).

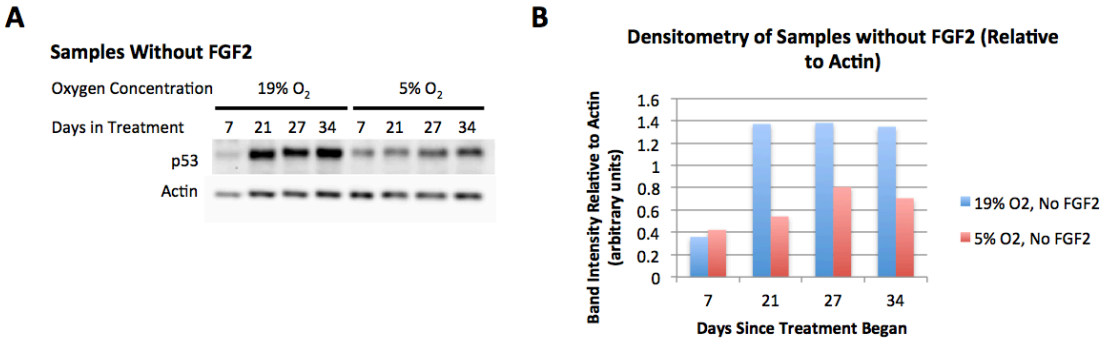

Figure 7.10 A) Western blot for p53 and actin control in cells not treated with FGF2. B) Densitometry quantification of p53 Western blot results for samples not treated with FGF2. Values are calculated relative to actin.

Lowering oxygen concentration in cells not treated with FGF2 lowers p53 protein levels. p53 protein accumulates at early passages in control cells and then remains relatively constant throughout the time course studied (Figure 7.10).

The quantification of the Western blots (Figure 7.9B and Figure 7.10B) supports the observations stated about the blots (Figure 7.9A and Figure 7.10A). Treatment with FGF2 appears to cause a reduction in p53 protein levels at the final time point after gradual accumulation, while the lower oxygen concentration lowers the protein levels overall.

7.4 Flow Cytometry

Cell cycle flow cytometry was performed on cell samples gathered and fixed in ethanol after 21 and 22 passages (No FGF2 and FGF2 samples, respectively). Signals recorded from the FL-2 channel were plotted as event count as a function of FL-2 intensity. All four samples show characteristic, bimodal distributions with an associated non-zero baseline between the peaks. The lower intensity peak in each plot represents the phase during which a cell is diploid (2n). This indicates cells in G_0 and G_1 phases of the cell cycle. The higher intensity peaks represent the period of

the cell cycle during which the cell is tetraploid. This occurs during the G_2 and M phases of the cell cycle. The portion of the plot below the non-zero connecting baseline represents cells with DNA content between diploid and tetraploid, during the S phase.

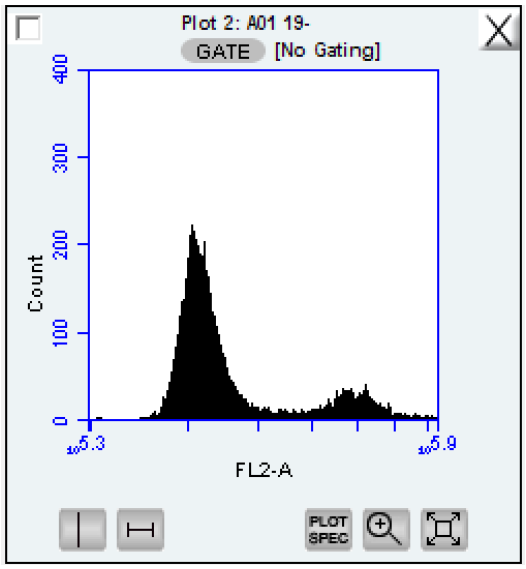

Figure 7.11 Flow cytometry results for 19% O2 cells, without FGF2, (control) at Passage 21.

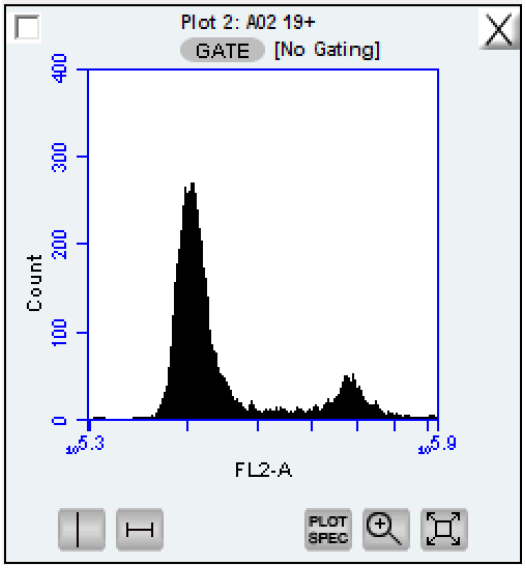

Figure 7.12 Flow cytometry results for 19% O2 cells, with FGF2, at Passage 22.

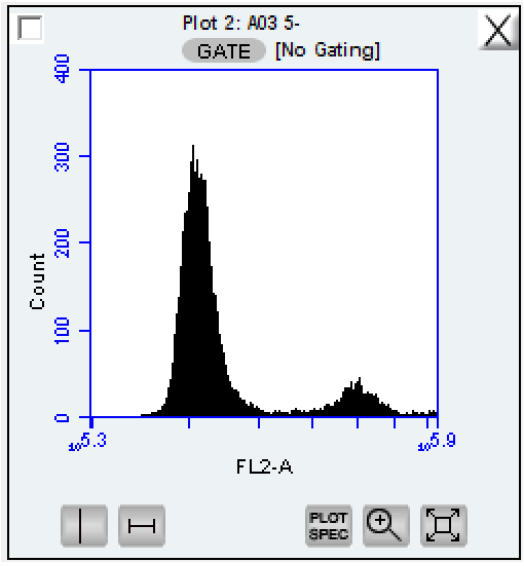

Figure 7.13 Flow cytometry results for 5% O2 cells, without FGF2, at Passage 21.

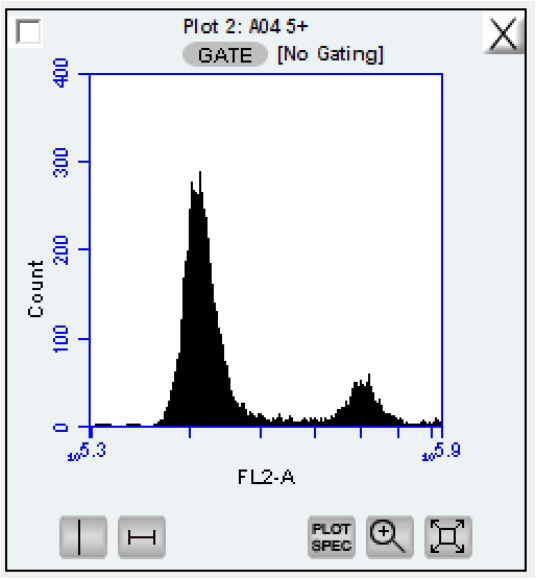

Figure 7.14 Flow cytometry results for 5% O2 cells, with FGF2, at Passage 22.

All four cell populations appear to have similar distributions of cells in each portion of the cell cycle (Figure 7.11, Figure 7., Figure 7.13, and Figure 7.14). The majority of cells appear to be in the G_0 or G_1 phases, with limited numbers in the S phase, and an intermediate amount of cells in the G_2 or M phases. At the time the cells were fixed in preparation for performing flow cytometry, the cells had undergone the following numbers of population doublings: 19% O_2 without FGF2, 34.28; 19% O_2 with FGF2, 41.09; 5% O_2 without FGF2, 29.08; 5% O_2 with FGF2, 36.08. The populations likely have not yet undergone senescence and, therefore, appear similar to each other.

8 Discussion

The addition of FGF2 and use of low oxygen concentration during culturing allows fibroblasts to undergo more population doublings in a shorter period of time before senescence than untreated fibroblasts in higher oxygen concentrations (Figure 7.1). p53 and p21 accumulate at the mRNA level in older, untreated cell populations. Growth at lower oxygen concentrations appears to maintain lower levels of mRNA for p53 and p21 and protein for p53 (Figure 7.3 and Figure 7.4). This may be related to the mechanism by which iRC cells postpone senescence. While p53 accumulates over time, it appears that it may be downregulated in later passage cells (Figure 7.3). p53 and p21 show similar trends in all cell populations, which is indicative of p21's downstream position in the p53 senescence pathway and suggests that p53 is active in all four cell populations (Figure 7.3 and Figure 7.4). p16 and MDM2 do not exhibit similar trends to either p53 or p21 (Figure 7.5 and Figure 7.6). MDM2 was not expected to follow the same trends as p53 because of its autoregulatory interaction with p53. This is also an illustration of p53's ability to differentially activate its transcriptional targets. p16 was tested for comparison of the effects of FGF2 and of lower oxygen concentration on p53 and an off-target senescence pathway. The difference in p16 and p53 transcript levels suggests that the differences observed in the different treatments were related to p53 and not reflected in all senescence pathways in the cells.

The protein experiments reflect the results of the RNA investigations (Figure 7.3, Figure 7.9, and Figure 7.10). The trends observed in each of the populations at the transcript level are similar to those shown in the Western blots and subsequent quantification. From these results, it can be concluded that the differences seen in p53 are likely due to transcriptional or post-transcriptional regulation mechanisms. Both FGF2 and lower oxygen concentration appear to have regulatory effects on p53 prior to production of the protein.

From the evidence gathered, it appears that supplementation of media with FGF2 lowers p53 levels. The same appears to be true of culturing cells at lower oxygen concentrations. Indirect lines in the network shown below indicate these findings. Direct lines show known interactions with p53 (Figure 8.1).

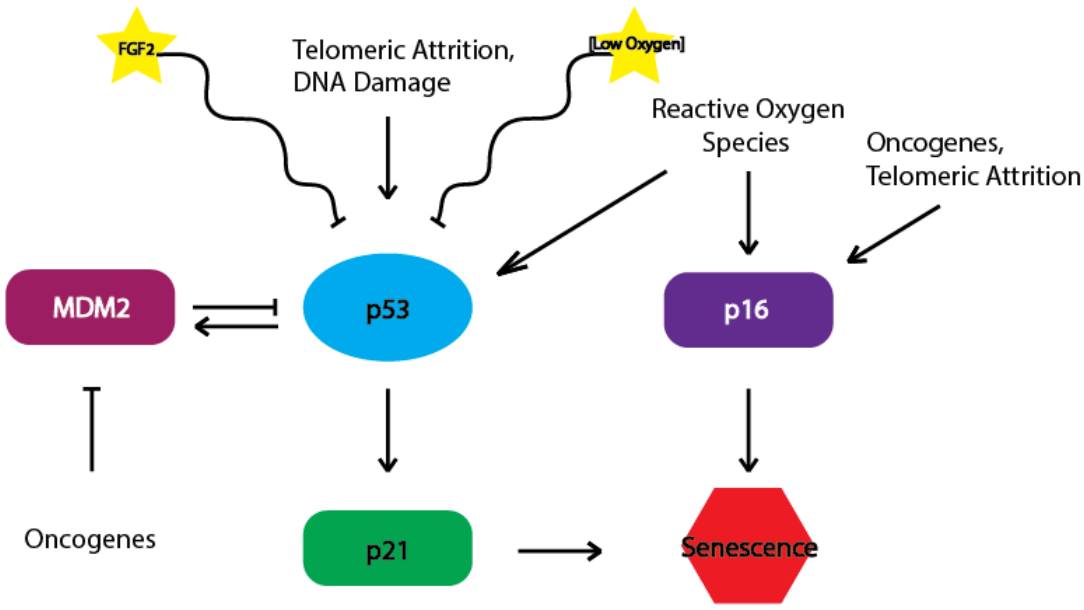

Figure 8.1 A schematic of proposed p53 interactions with studied proteins and under low oxygen and FGF2.

The experiments should be repeated, since this study only investigated these events once (n=1). Future studies should also include a longer time course for treatment of samples with FGF2 and low oxygen and additional biological replicates so statistical significance of the observed changes can be determined. The results of the RT-PCR, qRT-PCR, and protein studies are interesting, even before the expected senescence point of untreated fibroblasts, but the story would be more complete with the addition of later time points beyond the senescence point of untreated cells. Future projects could also include studies of localization of p53 transcripts or seek to identify possible additional post-translational modifications of p53.

9 References

Abraham, R. T. (2001). Cell cycle checkpoint signaling through the ATM and ATR kinases. *Genes Dev, 15*(17), 2177-2196. doi: 10.1101/gad.914401

Alberts, B., Johnson, A., Lewis, J., Raff, M., Roberts, K., & Walter, P. (2010). Molecular Biology of the Cell. New York: Garland Science; 2008. *Classic textbook now in its 5th Edition*.

Banin, S., Moyal, L., Shieh, S., Taya, Y., Anderson, C. W., Chessa, L., . . . Ziv, Y. (1998). Enhanced phosphorylation of p53 by ATM in response to DNA damage. *Science, 281*(5383), 1674-1677.

Bartek, J., & Lukas, J. (2001). Mammalian G1- and S-phase checkpoints in response to DNA damage. *Current Opinion in Cell Biology, 13*(6), 738-747. doi: http://dx.doi.org/10.1016/S0955-0674(00)00280-5

Brown, E. J., & Baltimore, D. (2000). ATR disruption leads to chromosomal fragmentation and early embryonic lethality. *Genes Dev, 14*(4), 397-402.

Canman, C. E., Lim, D. S., Cimprich, K. A., Taya, Y., Tamai, K., Sakaguchi, K., . . . Siliciano, J. D. (1998). Activation of the ATM kinase by ionizing radiation and phosphorylation of p53. *Science, 281*(5383), 1677-1679.

Cell Cycle Proteins. from National Center for Biotechnology Information

Chehab, N. H., Malikzay, A., Stavridi, E. S., & Halazonetis, T. D. (1999). Phosphorylation of Ser-20 mediates stabilization of human p53 in response to DNA damage. *Proc Natl Acad Sci U S A, 96*(24), 13777-13782.

Cooper, G. M. (2000). *The Cell: A Molecular Approach* (2nd ed.). Sunderland, MA: Sinauer Associates.

Counter, C. M., Avilion, A. A., LeFeuvre, C. E., Stewart, N. G., Greider, C. W., Harley, C. B., & Bacchetti, S. (1992). Telomere shortening associated with chromosome instability is arrested in immortal cells which express telomerase activity. *The EMBO journal, 11*(5), 1921.

Coutu, D. L., & Galipeau, J. (2011). Roles of FGF signaling in stem cell self-renewal, senescence and aging. *Aging (Albany NY), 3*(10), 920.

Falck, J., Mailand, N., Syljuasen, R. G., Bartek, J., & Lukas, J. (2001). The ATM-Chk2-Cdc25A checkpoint pathway guards against radioresistant DNA synthesis. *Nature, 410*(6830), 842-847.

Harper, J. W., Adami, G. R., Wei, N., Keyomarsi, K., & Elledge, S. J. (1993). The p21 Cdk-interacting protein Cip1 is a potent inhibitor of G1 cyclin-dependent kinases *Cell* (Vol. 75, pp. 805-816). United States.

Hayflick, L., & Moorhead, P. S. (1961). The serial cultivation of human diploid cell strains. *Experimental cell research, 25*(3), 585-621.

Herbert, B. S., Pitts, A. E., Baker, S. I., Hamilton, S. E., Wright, W. E., Shay, J. W., & Corey, D. R. (1999). Inhibition of human telomerase in immortal human cells

leads to progressive telomere shortening and cell death. *Proceedings of the National Academy of Sciences, 96*(25), 14276-14281.

Itahana, K., Campisi, J., & Dimri, G. P. (2004). Mechanisms of cellular senescence in human and mouse cells. *Biogerontology, 5*(1), 1-10.

Kashpur, O., LaPointe, D., Ambady, S., Ryder, E. F., & Dominko, T. (2013). FGF2-induced effects on transcriptome associated with regeneration competence in adult human fibroblasts. *BMC genomics, 14*(1), 656.

Kassem, M., & Marie, P. J. (2011). Senescence-associated intrinsic mechanisms of osteoblast dysfunctions. *Aging cell, 10*(2), 191-197.

Kastan, M. B., & Lim, D.-s. (2000). The many substrates and functions of ATM. *Nat Rev Mol Cell Biol, 1*(3), 179-186.

Molinari, M., Mercurio, C., Dominguez, J., Goubin, F., & Draetta, G. F. (2000). Human Cdc25 A inactivation in response to S phase inhibition and its role in preventing premature mitosis. *EMBO Reports, 1*(1), 71-79. doi: 10.1093/embo-reports/kvd018

Nakagawa, H., & Opitz, O. G. (2007). Inducing cellular senescence using defined genetic elements *Biological Aging* (pp. 167-178): Springer.

Nurse, P., Masui, Y., & Hartwell, L. (1998). Understanding the cell cycle. *Nat Med, 4*(10), 1103-1106. doi: 10.1038/2594

O'Connor, C. M., Adams, J. U., & Fairman, J. (2010). Essentials of Cell Biology. *NPG Education, Cambridge*.

Page, R. L., Ambady, S., Holmes, W. F., Vilner, L., Kole, D., Kashpur, O., . . . Dominko, T. (2009). Induction of stem cell gene expression in adult human fibroblasts without transgenes. *Cloning and stem cells, 11*(3), 417-426.

Pozarowski, P., & Darzynkiewicz, Z. (2004). Analysis of cell cycle by flow cytometry *Checkpoint Controls and Cancer* (pp. 301-311): Springer.

Rodier, F., & Campisi, J. (2011). Four faces of cellular senescence. *The Journal of cell biology, 192*(4), 547-556.

Ryan, K. M., Phillips, A. C., & Vousden, K. H. (2001). Regulation and function of the p53 tumor suppressor protein *Curr Opin Cell Biol* (Vol. 13, pp. 332-337). United States.

Sancar, A., Lindsey-Boltz, L. A., Unsal-Kacmaz, K., & Linn, S. (2004). Molecular mechanisms of mammalian DNA repair and the DNA damage checkpoints. *Annu Rev Biochem, 73*, 39-85. doi: 10.1146/annurev.biochem.73.011303.073723

Shaulian, E., Resnitzky, D., Shifman, O., Blandino, G., Amsterdam, A., Yayon, A., & Oren, M. (1997). Induction of Mdm2 and enhancement of cell survival by bFGF. *Oncogene, 15*(22), 2717-2725.

Stocum, D. L. (2002). Regenerative biology and medicine. *Journal of musculoskeletal & neuronal interactions, 2*(3), 270-273.

Takahashi, K., Okita, K., Nakagawa, M., & Yamanaka, S. (2007). Induction of pluripotent stem cells from fibroblast cultures. *Nature protocols, 2*(12), 3081-3089.

Takahashi, K., Tanabe, K., Ohnuki, M., Narita, M., Ichisaka, T., Tomoda, K., & Yamanaka, S. (2007). Induction of pluripotent stem cells from adult human fibroblasts by defined factors. *cell, 131*(5), 861-872.

Vijg, J., & Campisi, J. (2008). Puzzles, promises and a cure for ageing. *Nature, 454*(7208), 1065.

Wright, W. E., & Shay, J. W. (2002). Historical claims and current interpretations of replicative aging. *Nature biotechnology, 20*(7), 682-688.

Xu, B., Kim, S. T., Lim, D. S., & Kastan, M. B. (2002). Two molecularly distinct G(2)/M checkpoints are induced by ionizing irradiation. *Mol Cell Biol, 22*(4), 1049-1059.

Yu, J., Vodyanik, M. A., Smuga-Otto, K., Antosiewicz-Bourget, J., Frane, J. L., Tian, S., . . . Stewart, R. (2007). Induced pluripotent stem cell lines derived from human somatic cells. *Science, 318*(5858), 1917-1920.

Zhang, Y., & Xiong, Y. (2001). Control of p53 ubiquitination and nuclear export by MDM2 and ARF. *Cell Growth Differ, 12*(4), 175-186.

Zhao, H., & Piwnica-Worms, H. (2001). ATR-mediated checkpoint pathways regulate phosphorylation and activation of human Chk1. *Mol Cell Biol, 21*(13), 4129-4139. doi: 10.1128/mcb.21.13.4129-4139.2001